17th World Conference on Earthquake Engineering, 17WCEE
Sendai, Japan - September 13th to 18th 2020

EXPERIMENRAL STUDY ON DEFORMABILITY AND P-Δ EFFECT OF A WOODEN FRAMEWORK COMPRISEING STEEL LINTEL

A. Yamada[(1)]

[(1)] *Associate professor, Fukuyama University, yamada@fukuyama-u.ac.jp*
...

Abstract

A typical design plan for a Japanese wooden house comprises a 910 mm module with column intervals of 910-1,820 mm and beam spans of 3-4 m. In structural designs, ideally, the columns between the lower and the upper floors should be in the same location. However, such alignments do not often coincide in wooden houses because of the small rooms and their locations, which tend to create non-complementary alignment between the lower and upper floors. Therefore, the structures of wooden houses tend to be in disordered patterns as compared to other buildings with well-ordered placements of columns and beams.

The frameworks of two- or three-storied wooden houses sometimes have a framework with columns upstairs without any columns directly below. In such a framework, the supporting floor beams in the lower floor are designed such that there is no excessive vertical deflection, to allow the transmission of seismic force between the upper and lower floors. Therefore, large beams are used that cannot be contained above the ceiling. In such cases, wooden beams are sometimes replaced with steel beams.

Framework designs comprising mixed wood and steel are occasionally used in repairing existing wooden buildings. For example, when installing a new beam between two columns to support the vertical load, steel lintels are placed on the column side under the existing beams because the new beams interfere with existing floor beams.

Steel materials are generally reliable; however, solid and stable structures are unachievable without considering the difference in the material characteristics of steel and wood. This is particularly the case at joints that can be viewed as pin joints in steel structures but may behave as rigid joints in a mixed framework. Therefore, it is essential to pay considerable attention to the details of joints in frameworks comprising wood and steel.

In this study, we considered the installation of a new lintel between two columns in structures in which the column locations do not match between the upper and lower floors in existing wooden structures. The steel lintel is placed on the side of the wooden column to act as support to the vertical load. The joint between the wooden column and steel lintel is the experimental parameter, and we experimentally verified the horizontal deformability and strength of the structure and the behavior of the lintel-column joint.

The following findings were clarified from the experiments:

(1) The framework used in the experiment shows sufficient deformability, while no breakage of the column occurred until the story drift angle reached 1/10 rad.

(2) In the slip process of restoring the force characteristics, the horizontal stiffness of the structure was confirmed to become negative, resulting in P-Δ effect. A model and formulation are shown to demonstrate this effect.

(3) In general, in the event of any collapse of the wooden framework, the horizontal strength disappears because of relative-story displacement reaching the column width. However, in the framework used in this experiment, the horizontal strength was lost when the relative-story displacement reached half of the column width.

Keywords: Wooden Framework, Steel Lintel, Composite Structure, Horizontal Deformability, P-Δ Effect

1. Introduction

In the floor plan of a wooden house, the module is set to approximately 910 mm, the column spacing is 910–1820 mm, and the floor span of 3-4 m. Generally, in structural designs, it is desirable to align the locations of the columns between the top and bottom floors. In wooden frameworks, however, this alignment may not always be observed because partition walls are treated as load-bearing walls, although each of the rooms is small and their location does not align on the upper and lower floors. Therefore, these frameworks rarely have clear placements of columns and beams.

The frameworks of two- or three-storied wooden houses sometimes have a framework with columns upstairs without any columns directly below. In such a framework, the supporting floor beams in the lower floor are designed such that there is no excessive vertical deflection, to allow the transmission of seismic force between the upper and lower floors. Therefore, large beams are used that cannot be contained above the ceiling. In such cases, wooden beams are sometimes replaced with steel beams.

Composite frameworks are occasionally used in repairing existing wooden frameworks. An example for these is a case where a new beam is required between columns to support the vertical load; however a steel lintel is installed below the beam, i.e., it is centered in the direction of the column's height to avoid its interference with the existing floor system.

Steel materials are generally reliable; however, solid and stable structures are unachievable without considering the difference in the material characteristics of steel and wood. This is particularly the case at joints that can be viewed as pin joints in steel structures but may behave as rigid joints in a mixed framework. Therefore, it is essential to pay considerable attention to the details of joints in frameworks comprising wood and steel.

In this study, we considered the installation of a new lintel between two columns in structures in which the column locations do not match between the upper and lower floors in existing wooden structures. The steel lintel is placed on the side of the wooden column to act as support to the vertical load. The joint between the wooden column and steel lintel is the experimental parameter, and we experimentally verified the horizontal deformability and strength of the structure and the behavior of the lintel-column joint.

2. Outline of the experiment

2.1 Specimen

One specimen from each of the three types (No. 1-3) with parameters based on the difference in the connection specifications between wooden columns and steel lintels were manufactured. The main dimensions used include the following: a column center interval of 1820 mm and a column height (distance between the base and the beam center) of 2730 mm. The cross-sectional dimension of the column and base was 105×105 mm and that of the beam was 105×150 mm. The column-beam joint used was short tenon (section: 30×85 mm and depth: 50 mm) [1]-[2], with two metals attached to both sides of the column with a short-term tensile strength of 5.9 kN. The lintel used was a wide flange shapes H-100×100×6×8. The tree species of sill is Hinoki-cypress, the columns and beams are glued-laminated timber composed of symmetrical different grade (column: E95-F270, beams: E120-F330), and the steel is SS400. Figure 1 shows the framework of No. 1, and Figs. 2-3 shows the specifications of each lintel components.

The specifications of the connection are as follows: No. 1: Lag screw bolt, No. 2: Rib plate and No. 3: Base plate and gusset plate

No.1 is a specification based on an actual example. The column side is notched by 20 mm, the edge of the steel lintel is closed by 9 mm thick steel plate, and after that, the lintel is inserted into the column, and directly fixed with M12 and L = 75 mm lag screw bolt. The sectional loss of the column due to the notch was not different from that of the normal insertion, so it was judged to be acceptable.

No. 2 is a specification that does not have a notch in the column. It uses a metal fitting where a 6 mm thick rib plate is attached to an unequal leg angle L-150×100×9, and columns and lintels are fastened with

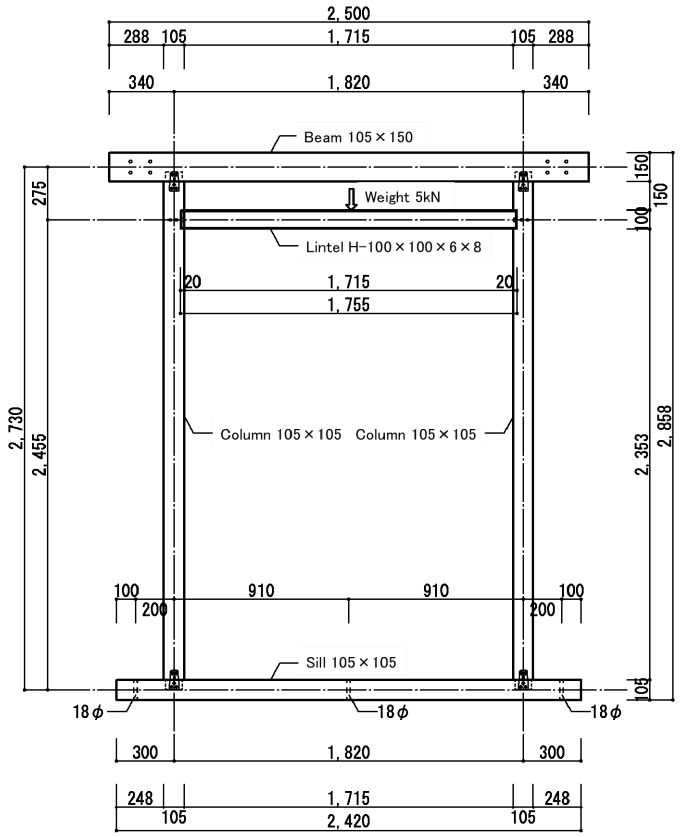

Fig. 1 – No. 1 Specimen frame diagram (this is the same for No. 2 and 3)

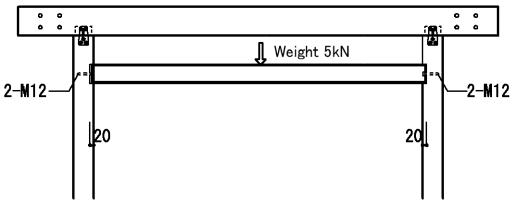

(a) No. 1

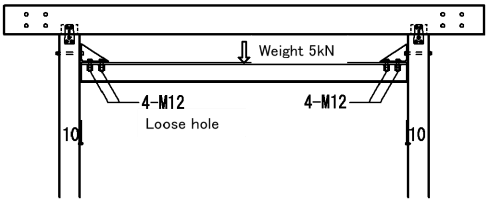

(b) No. 2

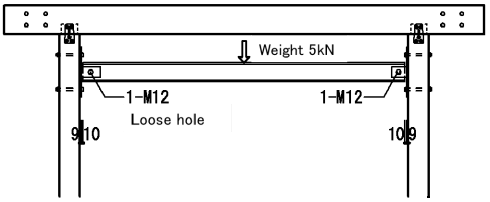

(c) No. 3

Fig. 2 – Specifications of the lintel

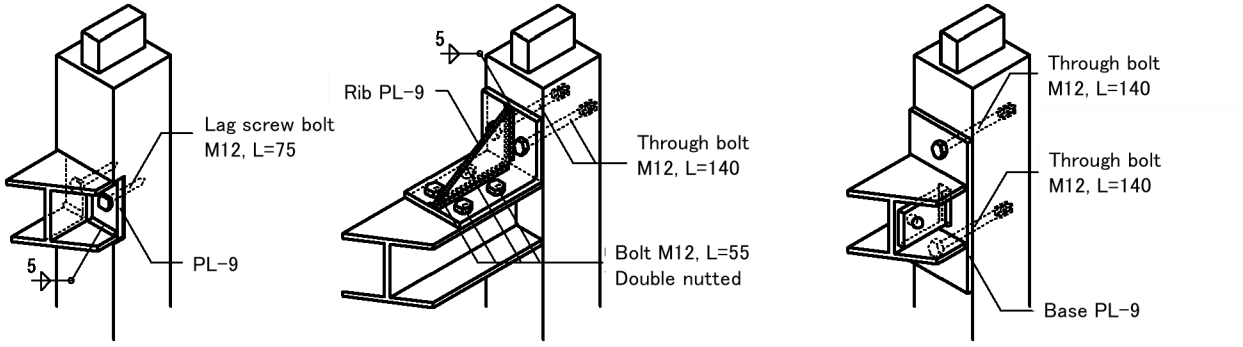

(a) No. 1 (b) No. 2 (c) No. 3

Fig. 3 – Specifications of lintel connection

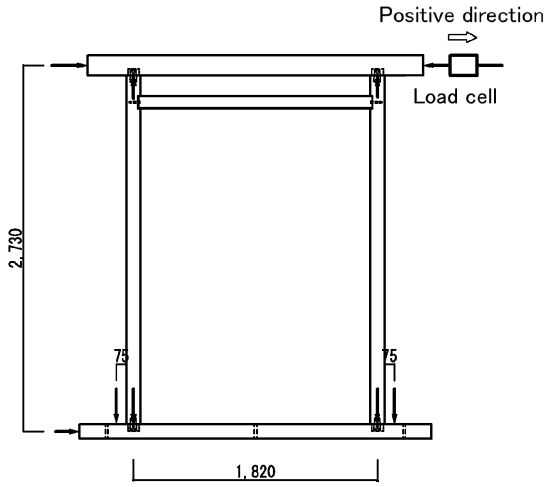

Fig. 4 – Displacement sensor location
(Arrow without note: displacement sensor)

Photo 1 – Installation of the weight (No. 1)

M12 bolts. In consideration of workability, the receiving bracket should be installed below the lintel so that we can temporarily receive lintels. However, it was assumed here that a sash or the like was provided below the lintel and the receiving bracket was installed above the lintel.

No. 3 specification was based on the steel structure, with the lintel bolted to a gusset plate fixed to the column with M12 bolts.

In No. 2 and 3, one end of the lintel was a loose bolt-hole and the other end was a normal bolt-hole for eliminating the dimensional error during construction.

2.2 Loading method

The base of the specimen was bound to a steel frame using anchor bolts, and the weight was attached to the center of the lintel as shown in Photo 1. In References [1] and [2], the vertical load was approximately 2,000 N/m; however, it was assumed to be a centralized load of 5 kN with reference to the actual structural calculation.

As seen at the top-right corner of Photo 1, a motor cylinder was placed at one end of the beam to apply an alternating load in the horizontal direction. The load cycle comprises apparent shear deformation angles

(horizontal displacement of the beam edge divided by height 2730 mm) of 1/450, 1/300, 1/200, 1/150, 1/100, 1/75, 1/50, 1/30, 1/15 and 1/10 rad, with the application of three cycles of positive and negative alternating forces.

2.3 Measurement method

Displacement transducers were placed at the butt end and side of the beam and at one end of the sill to measure the horizontal displacement of the specimen, and also at the four connections of the column edges to measure the slipping out the columns, and both ends of the sill to measure the vertical displacement. The installation positions are shown in Fig. 4.

3. Experimental results

3.1 Damage process

In No. 1, there was a deformation in the metal plate of the column joint at 1/40 rad, and a periodic squeaking sound was heard from the column joint between 1/200 and 1/10 rad. The sound gradually increased, achieving the maximum strength at 1/10 rad.

In No. 2, there was a periodic squeaking sound between 1/150 and 1/10 rad, which gradually increased. We observed the compressive strain on the column side due to the lintel at 1/12 rad, where the maximum bearing force was observed at 1/10 rad.

Similarly, in No. 3, there was a periodic squeaking sound between 1/100 and 1/10 rad, the metal plate of the column joint deformed at 1/30 rad, and a crack was observed at the column joint. Furthermore, a large deformation formed in the metal plate the column joint, and the maximum strength was observed at 1/10 rad.

No vertical displacement due to pulling out of column was observed in No. 1-3.; furthermore, in No. 2 and No. 3, deformation was observed in the bolt washer of the lintel on the column side.

3.2 Load-deformation relationship

Figures 5(a)-(d) show the relationship between the load and deformation and the corresponding envelope curve for No. 1-3, wherein Figs. 5(a)-(c) show that the stiffness of each specimen was negative during the slip process (broken lines in the figures). This was particularly obvious in No. 1 and 3 and can be attributable to the P-Δ effect. In the load-deformation relationship for a regular framework in another study [3], this phenomenon was not observed, despite the equivalent vertical load used.

The envelope curve for the positive applied force (first quadrant) shown in Fig. 5(d) indicates that the stiffness near the origins of No. 1-3 was approximately the same. Moreover, the strength characteristics of No. 1 and 2 were almost the same until approximately 1/15 rad (0.07 rad); however, the strength in No. 3 was approximately 0.6 times of that of No. 1 and 2. Furthermore, beyond 1/15 rad, the strength kept increasing in No. 2 and 3, whereas it plateaued in No. 1. One reason for this could be because when deformations is small resistance moment does not cause in the connection. As a result, resulting in little difference among the specimens No. 1-3. It seems that, when deformation was larger, resistance moment, which is created on the column side due to the lintel, started to increase in the lintel edge of No. 1 and in the angle edge of No. 2. On the other hand, No.3, which was the pin detail by a single bolt on the lintel edge, made it unlikely for resistance moment to occur at the connection.

The negative applied force (third quadrant) shown in the same figure indicates that the stiffness near the origin for No. 1-3 was approximately the same as the positive applied forces. Beyond that until 1/30 rad, the difference in the strength between No. 1-3 was not as clear as in the positive applied force; however, the two cases were qualitatively the same in the sense that the strength of No. 3 was the lowest. The strength of No. 1 almost reached the peak beyond 1/20 rad (0.05 rad), whereas it kept increasing for No. 2 and 3, which was also qualitatively the same as in the positive applied force.

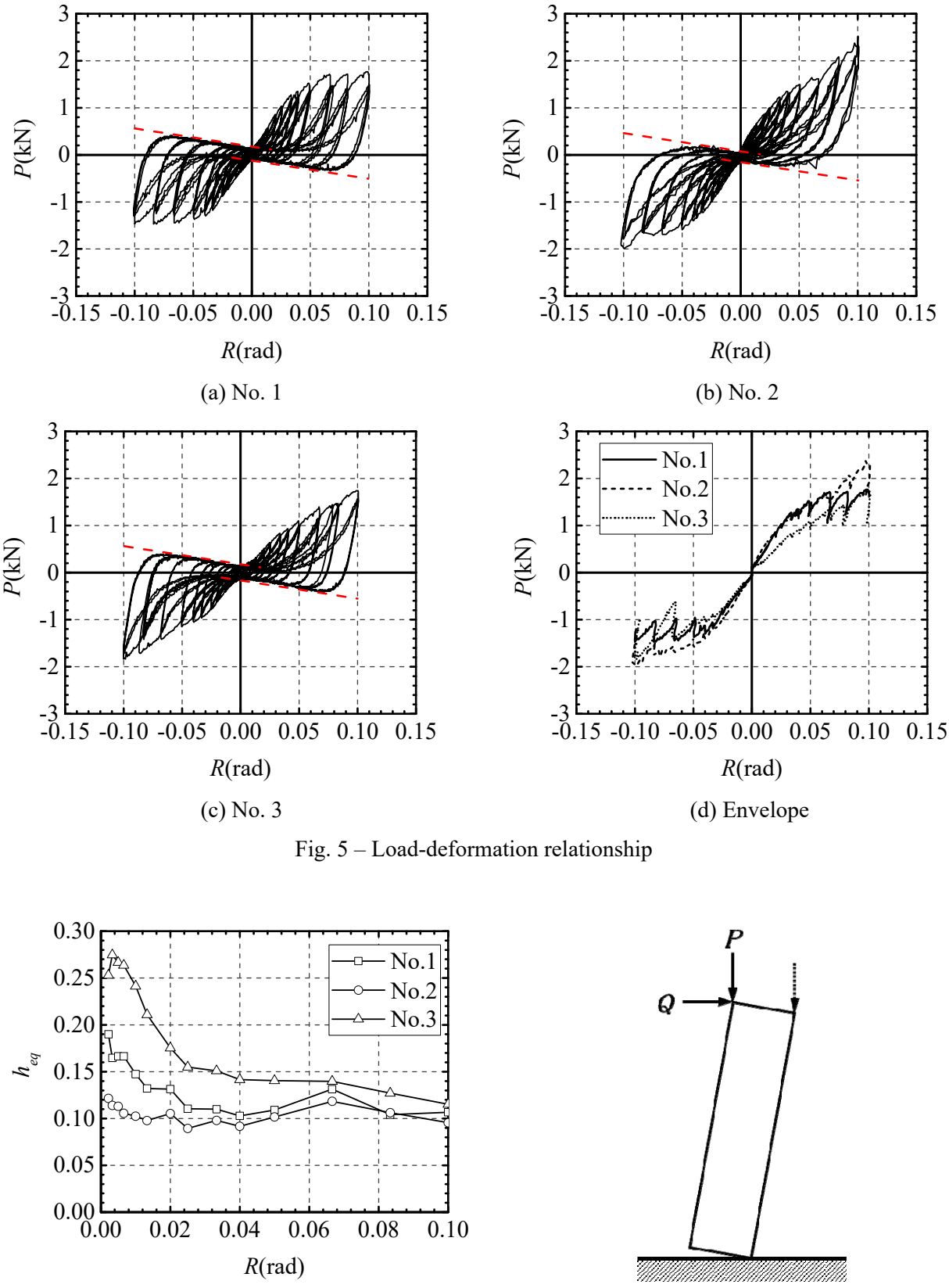

(a) No. 1 (b) No. 2

(c) No. 3 (d) Envelope

Fig. 5 – Load-deformation relationship

Fig. 6 – Equivalent viscous damping factor, h_{eq} Fig. 7 – Image of general column rocking resistance

The maximum strengths for No. 1, 2, and 3 were 1.76 kN, 2.37 kN, and 1.83 kN, respectively, with No. 2 having the highest value.

3.3 Equivalent viscous damping factor

Fig. 6 shows the equivalent viscous damping factor h_{eq} of No.1-3 calculated from the hysteresis loop of each deformation level of the first cycle. h_{eq} is calculated using the following formula in Eq. (1)

$$h_{eq} = \frac{1}{4\pi}\frac{\Delta W}{W} \tag{1}$$

where ΔW is the area of one hysteresis loop and W is the equivalent potential energy.

The figure shows that, until 1/20 rad, h_{eq} decreased with increasing drift angle for all specimens, subsequent to which the value converged around 12%. h_{eq} was the highest in No. 3, lowest in No. 2, and an intermediate value in No. 1.

When checking the shape of hysteresis loops, ΔW for each deformation level was the same for No. 1-3; however, W varied as the yield strength varied. This implies that h_{eq} was the highest for No. 3, wherein the yield strength was lowest. h_{eq} of the second and third cycle were about the same as that of the first loop in terms of the trend and values.

3.4 Wall ratio (Wall strength factor)

The walls in No. 1-3 were not bearing walls; however, when calculating the wall ratios, they were determined using the ultimate strength P_u or the strength at 1/120 rad and the values were approximately 0.1.

4. Observations of P-Δ effect

The P-Δ effect in wooden frameworks is well known along with the column rocking resistance. The column rocking resistance was first studied by Ban [4], studies conducted by Kawai [for example 5-6] resulted in it receiving considerable attention, subsequent to which several other researchers investigated it [for example 7-9]. In the practice of structural design, seismic diagnosis and seismic reinforcement, large diameter columns have been frequently considered [10-11]. The loss of the horizontal yield strength and reduced horizontal deformability due to the P-Δ effect is also widely known, and its effect is prominent in the design of interlaminar drift angles that are higher than 1/30 rad [12]. Experiments and theories suggest that a story shear coefficient of 0.2 corresponds to the loss of horizontal resistance at approximately 1/5 rad [13].

As shown in Fig. 7, existing studies on the P-Δ effect or restoring force to column rocking assumed that a vertical load P and horizontal load Q was applied on the column top. In this study, however, the lintel that supports the vertical load was attached to the side of the columns; therefore, the vertical load P was applied at the location of the dashed arrow in the figure. There are no previous studies on the P-Δ effect under such conditions, which is why a simple model was used.

As shown in Fig. 8 (a), a vertical load of $2P$ was applied at the center of the lintel, which is supported by the corner of the left and right columns. The columns on the left and the right are rigid bodies with the same cross-section with width B and height H. The column receives a horizontal load $2Q$, overturning by δ in the horizontal direction and by θ in the rotational angle.

For the columns to rotate and overturn around points D and D', as shown in Fig. 8(b), the overturning moment and stability moment should be

$$QH \times 2 \geq PB \tag{2}$$

Therefore, the horizontal force Q_0 necessary for the columns to start overturning is

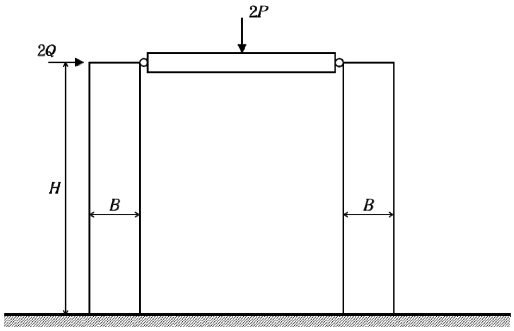

(a) Columns supporting a symmetric vertical load

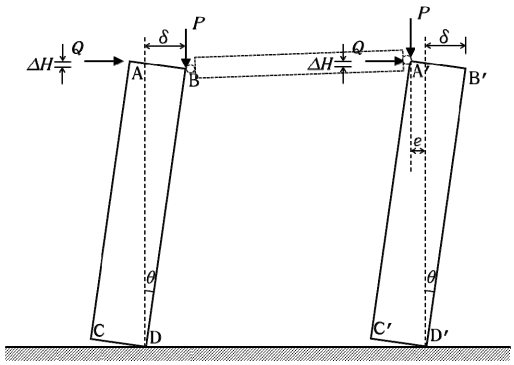

(b) Forces exerted on the left and right columns

(Before the vertical load *P* passes over point D')

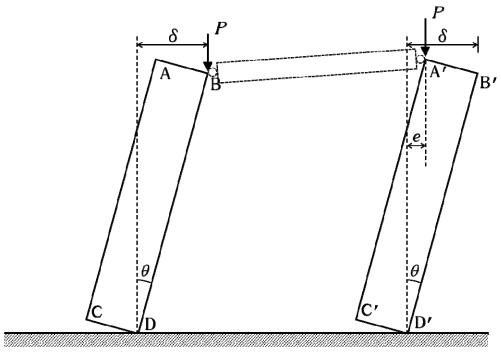

(c) Forces exerted on the left and right columns

(After the vertical load *P* passes over point D')

Fig. 8 – Rocking of the rigid columns supporting the beam at their corners

$$Q_0 = \frac{PB}{2H} \tag{3}$$

It was considered that the columns started to overturn and reached the condition shown in Fig. 8(b) when the vertical load *P* on the right passed over point D'.

Assuming that ΔH in the figure is sufficiently small, the total overturning moment M_T is

$$M_{\mathrm{T}} = Q(H+\Delta H)\times 2 + P\delta = 2QH + P\delta \tag{4}$$

The stability moment M_{O} is

$$M_{\mathrm{O}} = Pe = P(B\cos\theta - H\sin\theta) = P(B-\delta) \tag{5}$$

As M_{T} and M_{O} are balanced,

$$2QH + P\delta = P(B-\delta) \tag{6}$$

Therefore,

$$Q = \frac{P(B-2\delta)}{2H} = Q_0 - \frac{P\delta}{H} \tag{7}$$

When δ reaching $\delta = B/2$, Q becomes $Q = 0$.

When the load P passes over point D' as shown in Fig. 8(c), the overturning moment is given as

$$M_{\mathrm{T}} = P(\delta + e) = P\delta + P(\delta - B\cos\theta) = 2P\left(\delta - \frac{B\cos\theta}{2}\right) \tag{8}$$

and the columns overturn regardless of Q.

Figure 9 shows the simulation results of a case that neglected this assumption and a case that did not. The dotted line in the figure shows the load-deformation relationship due to the sweep excitation when the assumption was neglected. Three types of slip types and three perfect elasto-plastic types were combined [14], and the parameters were examined to match the general shape of the restoring force characteristics observed in the experiment. This resulted in the yield angles of perfect elasto-plastic type 1/240, 1/120 and 1/60, and each yield strength was 0.04 kN. The yield angles for the slip types were 1/30, 1/20 and 1/15 rad, and each yield strength was 0.56 kN. The solid line in the figure corresponds to the case which considered the assumptions on the P-Δ effect. The parameters used in Eqs. (2)-(8) were P=2.5 kN, $B = 105$ mm and $H = 2{,}603$ mm to be applicable for use in the experiment.

The solid line in the figure shows that the above-mentioned assumption led to an analytical reproduction of the experimental results, particularly the negative stiffness during the slip process. While in general rigid column rocking problems, the column rocking resistance vanished when $\delta = B$. In the frameworks studied in this study, the restoring force to column rocking vanished when $\delta = B/2$, indicating the early onset of the restoring force to column rocking.

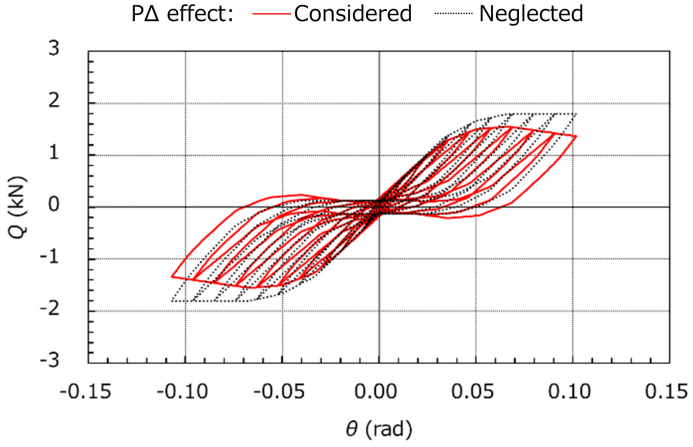

Fig. 9. Simulation of the P-Δ effect

5. Conclusions

In this study, the horizontal deformation performance of the composite framework of wooden frame and steel lintel was confirmed through experiments, assuming that a lower frame column is removed from a traditional wooden framed house, or that a vertical load is placed between the columns of an existing wooden houses. A model of the P-Δ effect was formulated for discussion based on the experiment. The conclusions obtained from the results are as follows.

(1) The three types of combined framework studied in the experiments all show sufficient deformation performance; there were no serious damages such as column fracture up to 1/10 rad, except for the deformation due to the compressive strain. From the viewpoint of yield strength, for No. 1 and 2 wherein resistance moment appeared at the lintel connection, the yield strength was higher than that of No. 3, which is closest to the pin connection. The difference in the connection details affected the yield strength. However, as these frames are not considered as bearing walls, every detail seems to be practical in the sense that it has sufficient deformability and no significant damage has occurred here.

(2) The P-Δ effect occurred when the hardness became negative during the slip process. A model for this phenomenon was formalized.

(3) The equivalent viscous damping factor decreased with the increasing drift angle, converging to approximately 12% beyond 1/20 rad.

(4) The wall ratio was approximately 0.1.

(5) With respect to (2), in general, the column rocking resistance vanishes when the horizontal displacement reaches the column width; however in the frameworks that have been investigated in this study, the column rocking resistance is lost at half the horizontal displacement, indicating an early onset of the P-Δ effect as compared with regular columns.

Acknowledgment

We thank the Kadosho Co., Ltd. for their support and cooperation in examining and preparing the specimens.

References

[1] Japan housing and wood technology center (2008): *Allowable stress design of wooden houses*.

[2] General building research corporation of Japan (2012), *Technical manual for the wall ratio of wooden bearing walls* (in Japanese)

[3] Yamada M, Suzuki Y, Goto M and Shimizu H (2004): Dynamic and static tests of wooden frames for evaluation of seismic performance. *Journal of structural and construction engineering (Transactions of AIJ)*, No. 582, 95-102 (in Japanese)

[4] Ban S (1941): Statics of building construction relating to Japanese temples and shrines (Part 1). *Transactions of AIJ*, No. 21, 252-258 (in Japanese)

[5] Kawai N (1991): A series of experiments on restoring force produced by rocking of wooden column, *Summaries of Technical Papers of Annual Meeting*, Architectural Institute of Japan, Structures-II, 91-92 (in Japanese)

[6] Kawai N (1993): Full-scale tests on restoring force of traditional wooden buildings produced by rocking of column and bearing wall, *Summaries of Technical Papers of Annual Meeting*, Architectural Institute of Japan, Structures-II, 1021-1022 (in Japanese)

[7] Kawai N (2017): Static loading test on column rocking resistance using scale models - In case of columns of square section -, *Summaries of Technical Papers of Annual Meeting*, Architectural Institute of Japan, Structures-III, 529-530 (in Japanese)

[8] Kawai N (2018): Static loading test on column rocking resistance using scale models Part 2. Influence of column section shape and theoretical solution considering initial deformation, *Summaries of Technical Papers of Annual Meeting*, Architectural Institute of Japan, Structures-III, 183-184 (in Japanese)

[9] Shibutani T, Takino A, Kunugi A and Miyamoto Y (2013): Horizontal load test and 3D finite element analysis of traditional wooden structure with rocking resistance, *Summaries of Technical Papers of Annual Meeting*, Architectural Institute of Japan, Structures-III, 423-424 (in Japanese)

[10] Kuramoto A, Kawai N, Nakagawa T, Sato T, Tsuwa I and Koshihara M (2018): Analytical study on seismic performances of a newly built five-storied pagoda Part2 Influence by restoring force characteristics considering tilt of column and P-Δ effect, *Summaries of Technical Papers of Annual Meeting*, Architectural Institute of Japan, Structures-III, 219-220 (in Japanese)

[11] Suda T, Tashiro Y, Mukaibo K and Suzuki Y (2011): Seismic reinforcement by restoring force due to column rocking for traditional wooden frame, *Journal of disaster mitigation for urban cultural heritage*, Ritsumeikan university, Vol. 5, 185-192 (in Japanese)

[12] Ministry of land, infrastructure, transport and tourism (2015), *Commentary on structural regulations of the building standard law of Japan* (in Japanese)

[13] Morii T, Miyamoto M, Yamada M and Hayashi Y (2010): Influence of P-Δ effects on deformation capacity of wooden frame structure, *Journal of structural and construction engineering (Transactions of AIJ)*, Vol. 75, No. 650, 849-857 (in Japanese)

[14] Yamada A, Suzuki S and Asano K (2004): A study on estimation of stiffness factor based on earthquake response characteristics of wooden-framed houses, *Journal of structural and construction engineering (Transactions of AIJ)*, Vol. 69, No. 584, 111-117 (in Japanese)

